CORA Cork Open Research Archive
Cartlann Taighde Oscailte Chorcaí

Title	A folate-targeted PEGylated cyclodextrin-based nanoformulation achieves co-delivery of docetaxel and siRNA for colorectal cancer
Authors	Zou, Yifang;Xiao, Fang;Song, Liu;Sun, Bingxue;Sun, Dandan;Chu, Di;Wang, Limei;Han, Shulan;Yu, Zhuo;O'Driscoll, Caitríona M.;Guo, Jianfeng
Publication date	2021-07-14
Original Citation	Zou, Y., Xiao, F., Song, L., Sun, B., Sun, D., Chu, D., Wang, L., Han, S., Yu, Z., O'Driscoll, C. M. and Guo, J. (2021) 'A folate-targeted PEGylated cyclodextrin-based nanoformulation achieves co-delivery of docetaxel and siRNA for colorectal cancer', International Journal of Pharmaceutics, 606, 120888 (9pp). doi: 10.1016/j.ijpharm.2021.120888
Type of publication	Article (peer-reviewed)
Link to publisher's version	10.1016/j.ijpharm.2021.120888
Rights	© 2021, Elsevier B.V. All rights reserved. This manuscript version is made available under the CC BY-NC-ND 4.0 license. - https://creativecommons.org/licenses/by-nc-nd/4.0/
Download date	2026-10-30 04:10:14
Item downloaded from	https://hdl.handle.net/10468/11738

UCC
University College Cork, Ireland
Coláiste na hOllscoile Corcaigh

A folate-targeted PEGylated cyclodextrin-based nanoformulation achieves co-delivery of docetaxel and siRNA for colorectal cancer

Yifang Zou [a #], Fang Xiao [b #], Liu Song [a], Dandan Sun [a], Di Chu [a], Limei Wang [c], Shulan Han [a], Zhuo Yu [d], Caitriona M O'Driscoll [e] *, Jianfeng Guo [a e] *

[a]School of Pharmaceutical Sciences, Jilin University, Changchun 130021, China

[b]Department of Pharmacy, the Second Hospital of Jilin University, Changchun 130041, China

[c]Department of Pharmacy, the General Hospital of FAW, Changchun 130011, China

[d]Department of Hepatopathy, Shuguang Hospital, Affiliated to Shanghai University of Traditional Chinese Medicine, Shanghai 201203, China

[e]Pharmacodelivery Group, School of Pharmacy, University College Cork, Cork T12 YT20, Ireland

#These authors are joint first authors.

*Corresponding authors:

Email: jguo@jlu.edu.cn (J Guo), caitriona.odriscoll@ucc.ie (CM O'Driscoll).

Abstract

Colorectal cancer (CRC) is one of the world's most lethal diseases. Docetaxel (DTX) is a chemotherapeutic agent used for a range of cancers, but it has little activity against CRC. However, combination therapy with other therapeutic agents is a potential strategy to enhance the efficacy of DTX in CRC treatment. The nuclear factor-κB (NF-κB) signaling pathway is implicated in a variety of malignancies (e.g., CRC), and the blockade of NF-κB may increase the sensitivity of cancer cells to chemotherapy. The application of small interference RNA (siRNA) to inhibit the translation of complementary mRNA has demonstrated the potential for cancer gene therapy. In this study, an amphiphilic cationic cyclodextrin (CD) nanoparticle modified with PEGylated folate (FA; a ligand to target folate receptor on CRC) has been developed for co-delivery of DTX and siRNA (against the RelA, a subunit of NF-κB) in the treatment of CRC. The resultant co-formulation (CD.DTX.siRelA.PEG-FA) achieved cell-specific uptake indicating the function of the folate targeting ligand. The CD.DTX.siRelA.PEG-FA nanoparticle enhanced the apoptotic effect of DTX with the downregulation of RelA expression, which significantly slowed down the growth of CRC in mice relative to the counterparts containing either DTX or siRelA, without causing significant toxicity. These results suggest that the folate-targeted PEGylated CD-based co-formulation provides a promising strategy for combining DTX and siRNA in treating CRC.

Keywords: colorectal cancer, nanoparticle, chemotherapy, gene therapy, combination therapy.

1. Introduction

Colorectal cancer (CRC) is one of the most common malignancies, with an estimated increase in the number of new incidents worldwide, from 1.8 million in 2018 to 25 million in 2035 (Dekker et al., 2019) (Bray et al., 2018). While surgery and radiation therapy are applied for localized CRC, chemotherapy remains the mainstay of clinical practice for patients at advanced or recurrent stages (Gustavsson et al., 2015). Docetaxel (DTX), marketed under the brand name Taxotere®, is known as a chemotherapy drug used for a range of cancers; however, it is less effective in the treatment of CRC (Sternberg et al., 1994) (Pazdur et al., 1994). Emerging evidence reveals that combination with other therapeutic agents may enhance the efficacy of chemotherapy drugs (Labala et al., 2017) (Joshi et al., 2020) (Nikkhoo et al., 2020). Therefore, the development of combination therapy presents excellent potential to improve the efficacy of DTX for CRC.

The nuclear factor-κB (NF-κB, a family of inducible transcription factors) signaling pathway is activated in a variety of cancers. It is implicated with the resistance of cancer cells to chemotherapeutics (Taniguchi and Karin, 2018). It has been reported that the NF-κB signaling pathway plays a crucial role in the maintenance of DTX resistance, and the blockade of this pathway can enhance the susceptibility of cancer cells to DTX (Kim et al., 2009) (O'Neill et al., 2011). The application of small interference RNA (siRNA) to exert downregulation of complementary mRNA achieves sequence-specific post-transcriptional gene silencing *in vitro* and *in vivo* (Guo et al., 2010) (Guo et al., 2011), suggesting that the combination of anti-NF-κB siRNA may improve the efficacy of DTX in the treatment of CRC.

Recently, the design and formulation of nano delivery constructs for transporting

chemotherapy drugs, nucleic acids, and peptides/proteins have significantly overcome the barriers to *in vitro* and *in vivo* delivery (Guo and Huang, 2020). Previously, an amphiphilic cationic β-cyclodextrin (CD, Fig. 1A) has been developed in our laboratories for delivery of siRNA in a range of cell lines (Fitzgerald et al., 2015) (Guo et al., 2017) and animal models (Godinho et al., 2013) (McCarthy et al., 2013). It is hypothesized that DTX and siRelA may be co-encapsulated within the CD nanoparticle (NP) due to the availability of various loading domains including: the hydrophobic CD cavity facilitating inclusion complex formation, the lipid domain and the cationic nature of the amphiphilic cationic CD. In this study, a folate-targeted PEGylated CD-based co-formulation (namely CD.DTX.siRelA.PEG-FA) was developed to deliver DTX and siRelA specifically to CRC cells *via* the folate receptor (a molecule found on the surface of CRC cells). The resultant co-formulation achieved significantly higher cellular uptake compared to the non-targeted counterpart, and improved the apoptotic efficacy of DTX with a reduction in the expression of RelA mRNA and protein, resulting in a synergistic anticancer effect in a mouse CRC model.

2. Materials and methods

2.1. Materials

Docetaxel (DTX) was purchased from DESITE Biotech. Negative control siRNA (siNC) (sense sequence 5'-UUC UCC GAA CGU GUC ACG U-3'), FAM-labelled siNC (siFAM) (modified with carboxyfluorescein (FAM) on sense sequence), and anti-RelA siRNA (siRelA) (sense sequence 5'-CCA UCA ACU AUG AUG AGU U-3') were purchased from GenePharma. 1,2-distearoyl-sn-glycero-3-phosphoethanolamine-N-[methoxy(polyethylene glycol)-2000] (DSPE-mPEG2000) was obtained from NANOCS, and 1,2-distearoyl-sn-glycero-3-phosphoethanolamine-N-

[folate(polyethylene glycol)-2000] (DSPE-PEG2000-Folate) was obtained from Avanti. The other reagents were purchased from Sigma-Aldrich unless mentioned otherwise. The amphiphilic cationic β-cyclodextrin (CD) was synthesized, as previously reported (O'Mahony et al., 2012).

2.2. Co-formulation preparation

Briefly, to prepare folate-targeted co-formulation (Fig. 1A), the CD was dissolved in trichloromethane with DTX and evaporated to form a thin film. This content was rehydrated, sonicated for 20 min, and incubated at 37 oC with slight shaking for 2 to 3 h, resulting in the CD.DTX NP. As previously reported (Evans et al., 2016), DSPE-mPEG2000 and DSPE-PEG2000-FA (molar ratio = 4:1) were dissolved in 20 mM HEPES buffer (pH = 7.4) and incubated at 60 °C for 15 min to obtain a solution (0.5 mg/mL). Subsequently, the DSPE-mPEG2000/DSPE-PEG2000-FA solution was added to CD.DTX and incubated at 60°C with slight shaking for one hour, in order to achieve the CD.DTX.PEG-FA NP (~ 2 mol% of FA in the outer surface per NP in theory). The CD.DTX.PEG-FA was then incubated with siRNA at room temperature for 30 min to form the folate-targeted co-formulation. The non-targeted and non-PEGylated co-formulations were prepared as described above without the use of DSPE-mPEG2000 and DSPE-mPEG2000/DSPE-PEG2000-FA, respectively.

2.3. Physicochemical profiles

The encapsulation efficiency (EE) and loading capacity (LC) of DTX were determined using HPLC (Shimadzu, Japan) (C18 column; UV at 227 nm; with a mobile phase of acetonitrile and water, v/v = 60:40). The EE% = (weight of encapsulated DTX/weight of feed DTX) x 100%; the LC% = (weight of encapsulated DTX/weight of total formulation) x 100%. The complexation of siRNA (0.5 μg) by CD.DTX,

CD.DTX.PEG and CD.DTX.PEG-FA was assessed by gel electrophoresis in 1% (w/v) agarose gel at 120 V for 30 min in Tris/Borate/EDTA buffer containing GelStain (Transgen Biotech) (Guo et al., 2012b).

The morphology of folate-targeted co-formulation was examined by transmission electron microscopy (TEM). Briefly, a sample containing 100 μg CD were added to a 400-mesh carbon-filmed copper grid (Agar Scientific) for 2 min. The sample was then stained with 2% (w/w) uranyl acetate, before analysis using JEOL JEM-1230.

The size distribution and zeta potential of co-formulations were measured using Malvern Nano-ZS as previously reported (Guo et al., 2012a). In addition, the effect of serum-containing media on the stability of co-formulations was assessed by incubating co-formulations within 50% fetal bovine serum (FBS) for 24 h at 37oC. The particle sizes were measured by Malvern Nano-ZS to determine the NP stability.

To perform drug release study, the folate-targeted co-formulation solution containing 500 μg DTX within a dialysis bag (MWCO = 2 kDa; Solarbio®) was incubated in the release medium (0.01 M PBS containing 0.5% Tween 80; pH values = 5.5 and 7.4) at 37℃ with slight stirring. At different time points, the supernatant was collected, and the release medium with the same volume was supplemented. The concentration of DTX in the supernatant was measured using HPLC as described above.

2.4. *In vitro* characterization

CT26 cells (a mouse CRC cell line expressing folate receptor (Fani et al., 2012)) were maintained in RPMI 1640 medium with 10% FBS and 1% Penicillin-Streptomycin at 37 oC with 5% CO2 and 95% relative humidity.

CT26 cells (200,000 per well) were seeded in 6-well plates. Following 24 h incubation, cells were treated with CD.DTX.siFAM.PEG or CD.DTX.siFAM.PEG-FA

([C] of siFAM = 25 nM) and incubated for 4 h. Subsequently, cells were washed with PBS and trypsinized. After the centrifugation at 1000 rpm for 5 min, cells were resuspended in 500 μL of ice-cold PBS and analyzed using flow cytometry (Becton Dickinson FACSCalibur) to determine FAM-positive cells (%).

The cytotoxicity was studied using the MTT assay. Briefly, CT26 cells were seeded at a density of 5 × 103 cells per well in 96-well plates for 24 h. Subsequently, free DTX or DTX encapsulated within co-formulations were added into the cells for 24 h. After this, cells were added with 20 μL of MTT reagent (5 mg/mL in PBS) and incubated at 37 oC for four hours. The purple precipitate was dissolved by 150 μL of DMSO before the measurement at 570 nm using Microplate Reader.

CT26 cells (200,000 per well) were seeded in 6-well plates for 24 h. Subsequently, free DTX or DTX encapsulated within co-formulations were added into the plates for 24 h. According to the manufacturer's instructions, cells were then treated with Annexin V-FITC and propidium iodide (PI) (YEASEN Biotech). Apoptotic cells (%) were determined using flow cytometry.

CT26 cells (50,000 per well) were seeded in 24-well plates for 24 h. Subsequently, co-formulations containing siRNA ([c] = 25 nM) were added into cells for 24 h. Total RNA was isolated using the TransZol up kit (TransGen Biotech). First-strand cDNA was generated using the TransScript® First-Strand cDNA Synthesis SuperMix kit (TransGen Biotech). qPCR was performed by the StepOnePlusTM Real-Time PCR System (ThermoFisher) using the TransStart® Top Green qPCR SuperMix kit (TransGen Biotech). The assay was performed using appropriate primers for RelA and GAPDH (Table S1) under thermal conditions as previously described (Luan et al., 2019).

CT26 cells (50,000 per well) were seeded in 24-well plates for 24 h. Subsequently, co-formulations containing siRNA ([c] = 25 nM) were added into cells for 24 h. CT26 cells were then lysed using the RIPA Lysis Buffer (Beyotime Biotech) containing 1 mM PMSF (Beyotime Biotech). The concentration of proteins was quantified using the BCA assay (TransGen Biotech). After this, ~ 30 to 45 μg samples were loaded into the SDS-polyacrylamide gel and electrophoresed at 80 V for 30 min and subsequently 120 V for o. Proteins were then transferred onto a polyvinylidene fluoride (PVDF) membrane (Invitrogen) at 90 V for 1.5 h. The membrane was incubated overnight with appropriate antibodies (Table S2) at 4℃. The secondary antibody (Table S2) was added to the membrane for 1.5 h. Proteins were detected using the enhanced chemiluminescence (ECL) solution (YEASEN Biotech) and quantified using ImageJ.

2.5. *In vivo* studies

Six to eight-week-old female BALB/C mice were obtained from Changchun Institute of Biological Products, China. The experiments have been approved by the Animal Ethics Committee of Jilin University.

Healthy mice (n = 4) were intravenously (i.v.) injected with folate-targeted co-formulation containing DTX (~ 4 mg/kg) and siRelA (~ 1 mg/kg) on Day 1, 3 and 5. Bodyweight was regularly recorded. On Day 25, major organs and the serum were obtained to analyze histopathology, myelosuppression, and hepatic/renal functions as previously described (Guo et al., 2020).

The mouse CRC model was established by subcutaneous injection of 5 × 105 CT26 cells into the animal flank. The tumor volume was calculated using the formula a2b(π/6), where a is the minor diameter of the tumor and b is the major diameter perpendicular to diameter a. When the tumor volume reached ~ 150 mm3 (Day 0), mice

(n = 5) were i.v. injected with co-formulations containing DTX (~ 4 mg/kg) and siRelA (~ 1 mg/kg) on Day 1, 3 and 5. The tumor growth was recorded regularly. Separately, two days after three injections (Day 7), tumors were collected for the following studies: 1) For apoptosis, tumors (n = 3) were fixed with 4% paraformaldehyde (PFA), conducted on paraffin-embedded slides, and permeabilized (Yu et al., 2020). Apoptotic cells were examined using the TransDetect® *In Situ* Fluorescein TUNEL Cell Apoptosis Kit (TransGen Biotech), and nuclei were stained with DAPI (Beyotime Biotech), for confocal microscopic analysis (Olympus, FV3000). 2) For the expression of RelA mRNA, tumors (n = 4) were homogenized within TransZol Up reagent (TransGen Biotech) using the tissue grinder (Scientz, China). The homogenate was centrifuged at 12,500 rpm for 20 min at 4 oC to collect the supernatant for RT-qPCR as described above. 3) For the expression of RelA protein, tumors (n = 4) were homogenated within the RIPA Lysis Buffer (Beyotime Biotech) containing 1 mM PMSF (Beyotime Biotech) using the tissue grinder (Scientz, China). The homogenate was centrifuged at 12,500 rpm for 20 min at 4 oC to collect the supernatant for western blotting as described above.

2.6. Statistical Analysis

GraphPad prism was applied for statistical analysis. Values were calculated as mean ± standard deviation (SD). A one-way ANOVA (Bonferroni's Post-Hoctest) was used to test the significance of differences in three or more groups. A two-way ANOVA (Bonferroni's Post-Hoctest) was used to test the significance of differences in the analysis of body weight and tumour growth. In all experiments, $p < 0.05$ was considered statistically significant.

3. Results and Discussion

3.1. Physicochemical Characterization of folate-targeted co-formulation

To provide a strategy that improves the efficacy of DTX against CRC, a folate-targeted PEGylated CD-based co-formulation was developed in this study by co-encapsulating DTX and siRelA into the CD with PEGylated FA to target the folate receptor on CRC cells (Fig. 1A). The HPLC results show that DTX was encapsulated inside the CD at different weight ratios (WR) of CD and DTX (Table S3). At WR5 between CD and DTX, the EE and LC were ~ 92% and ~ 15.3 wt %, respectively (Table S3). Due to the favorable EE and LC, the WR5 of CD and DTX was used for the preparation of the co-formulations.

It is known that DTX is poorly solube in water (2.903 μg/mL) and is given to patients as Taxotere® in a mix of Polysorbate 80 and ethanol (50:50, v/v) as a solvent (Huang et al., 2011). However, this solvent can cause adverse effects such as myelosuppression, hypersensitivity reaction, hemolysis, and fluid retention (Ferraresi et al., 2000) (Esmaeli et al., 2001). Consequently, a variety of formulations have been developed to improve solubility of DTX (Quaglia et al., 2009) (Esmaeili et al., 2008) (Liu et al., 2010) (Ferrati et al., 2015) (Bowerman et al., 2017) (Wang et al., 2017) (Chi et al., 2019). For example, hydroxypropyl-sulfobutyl-β-cyclodextrin (HP-SBE-β-CD) due to inclusion complex formation with DTX, achieved a LC of ~ 5.6 wt% (Huang et al., 2011). In addition, 2-hydroxypropyl β-cyclodextrin (HPCD) formed inclusion complexes with DTX resulting in a LC of ~ 5.2 wt% (Ferrati et al., 2015). In comparison, the LC of DTX was significantly improved by our CD (~ 15.3 wt%, Table S3) formulation. This is likely due to the combined availability of various loading domains including; the hydrophobic CD cavity facilitating inclusion complex formation, and the lipid domain of the amphiphilic cationic CD (Fig. 1A).

The modification of PEG and PEG-FA onto the CD.DTX was achieved using the

"postinsertion" technique (Fig. 1A and Table S4). This versatile approach allows the incorporation of PEG and targeting ligands into a variety of preformed liposomes or liposome-like structures (Rothdiener et al., 2010) (Evans et al., 2017). Subsequently, the capacity of CD.DTX, CD.DTX.PEG, and CD.DTX.PEG-FA to complex siRNA was assessed using gel retardation. Results show that siRNA was complexed onto CD.DTX *via* electrostatic interaction between the CD and siRNA, and the full complexation occurred at WR20 of CD and siRNA (Fig. S1). The binding of siRNA was also fully achieved by CD.DTX.PEG and CD.DTX.PEG-FA at WR20 of CD and siRNA (Fig. 1B), indicating that the ability of the CD to complex siRNA remained unaffected by the modification of PEG and PEG-FA (WR5 of CD and PEG-(FA)).

The dynamic light scattering (DLS) results show that CD.DTX.siRNA.PEG and CD.DTX.siRNA.PEG-FA demonstrated significantly larger particle sizes (122 and 125 nm, respectively) as compared to CD.DTX.siRNA (~ 100 nm) (Fig. 1C), indicating the successful incorporation of PEG and PEG-FA. The polydispersity index (PDI) of CD.DTX.siRNA, CD.DTX.siRNA.PEG and CD.DTX.siRNA.PEG-FA was 0.24, 0.26 and 0.27 respectively (Fig. 1C), indicating the generation of mainly monodisperse co-formulations. In addition, while the CD.DTX.siRNA displayed a significant cationic surface charge (40 mV), the surface charge of CD.DTX.siRNA.PEG and CD.DTX.siRNA.PEG-FA remained nearly neutral (9 mV and 10 mV, respectively) (Fig. 1C), likely due to the steric interference from PEG and PEG-FA (Rahme et al., 2015). Compared to CD.DTX.siRNA (EE ≈ 92% and LC ≈ 15%), CD.DTX.siRNA.PEG and CD.DTX.siRNA.PEG-FA achieved similar EE (~ 90% and 89%, respectively) and LC efficiencies (~ 12.2% and ~ 11.8%, respectively) (Fig. 1C), indicating that the capacity of CD to encapsulate DTX also remained unaffected by the modification of PEG and PEG-FA. The TEM results show that a spherical structure was formed by

CD.DTX.siRNA.PEG-FA (Fig. 1D), which was similar to the morphologies observed by CD.DTX.siRNA and CD.DTX.siRNA.PEG (data not shown). Due to favorable physicochemical profiles (Fig. 1B and 1C), WR5 of CD and DTX, WR20 of CD and siRNA, and WR5 of CD and PEG/PEG-FA (~ 2 mol% of FA per NP in theory) were used for the preparation of co-formulations.

The release efficiency of DTX from folate-targeted co-formulation was evaluated under different pH conditions (Fig. 1E). Results show that > 90% of DTX was released at 24 h in an acidic environment (pH 5.5), while the release efficiency of DTX was significantly reduced (~ 40%, $p < 0.05$) in the neutral environment (pH 7.4). These results imply that the co-formulation may achieve a higher DTX release in an acidic environment, which is similar to other amine-functionalized NPs that also facilitate pH-sensitive drug release (Gao et al., 2010) (He et al., 2017). We have previously demonstrated that siRNA was released from the CD inside endosomes (pH ≈ 5.5 to 6.0) due to the presence of the amine moiety inducing the proton sponge effect (Guo et al., 2017) (Fitzgerald et al., 2016a). Taken together, this data suggest that when folate-targeted co-formulation targets CRC cells *via* the folate receptor and subsequently enters into the endosome, DTX and siRNA can be simultaneously released into the cytoplasm to elicit a synergistic therapeutic effect (see below discussion).

It is known that PEGylation has been used as a stabilizing ligand to form so-called "stealth" NP for enhancing pharmacokinetic profiles (Suk et al., 2016). When incubated in 50% serum-containing medium for 24 h, the particle size of the PEGylated co-formulations, CD.DTX.siRNA.PEG and CD.DTX.siRNA.PEG-FA, was in the range of ~ 120 to 125 nm (Fig. 1F). In contrast, the diameter of non-PEGylated co-formulation, CD.DTX.siRNA, was significantly greater (> 750 nm, $p < 0.05$) under the same conditions (Fig. 1F). This data indicate the capacity of the PEG groups to efficiently

mask the surface charge of the co-formulations and improve stability in the presence of serum, suggesting the potential to extend blood circulation times. Due to instability, CD.DTX.siRNA was not used in the following *in vitro* and *in vivo* studies.

3.2. *In vitro* studies of folate-targeted co-formulation

The antiproliferative property of the co-formulations was studied in the CT26 cell line (a mouse CRC cell line expressing the folate receptor (Fani et al., 2012)) using an MTT assay. It is interesting to note that DTX on its own caused ~ 20% cell death (IC20) at 1.33 μg/mL (Fig. S2 and S3), and no significant difference in the cytotoxicity was achieved by CD.DTX.PEG containing DTX at the same concentration (Fig. S3). In contrast, CD.DTX.PEG-FA containing DTX at 1.33 μg/mL significantly ($p < 0.05$) increased the antiproliferative effect (~ 40% cell death) compared to free DTX and CD.DTX.PEG (Fig. S3). In addition, CD.siRelA.PEG-FA generated significantly higher cell death (~ 20%, $p < 0.05$) as compared to CD.siRelA.PEG and CD.siNC.PEG-FA (Fig. S4), due possibly to the cell-specific delivery of DTX and siRelA *via* the ligand-receptor pathway.

Subsequently, FAM-labeled siRNA was used to investigate the uptake of co-formulations in CT26 cells (Fig. 2A). No internalization was observed by siFAM alone as compared to untreated control. In contrast, the uptake of siFAM complexed within the non-targeted co-formulation was significantly higher ($p < 0.05$) than free siFAM (Fig. 2A and S5), while the folate-targeted co-formulation further ($p < 0.05$) increased the internalization of siFAM into CT26 cells (Fig. 2A and S5). These results confirm the capacity of the folate targeting ligand to promote receptor specific uptake.

In addition, the folate-targeted co-formulation containing the combination of DTX and siRelA caused significantly higher cytotoxicity (~ 95%, $p < 0.01$) as compared to non-targeted counterpart (~ 40%) (Fig. 2B), indicating that the antiproliferative activity

resulted mainly from cell-specific delivery of DTX and siRelA. Moreover, the cytotoxic effect of CD.DTX.siRelA.PEG-FA was significantly greater ($p < 0.01$) than either CD.DTX.PEG-FA or CD.siRelA.PEG-FA (Fig. 2C), indicating the synergistic therapeutic response from the combination of DTX and siRelA. CD.DTX.siRelA.PEG-FA also led to a synergistic apoptotic effect (~ 95%, $p < 0.01$) in CT26 cells relative to CD.DTX.PEG-FA (~ 18%) or CD.siRelA.PEG-FA (~ 8%) (Fig. 2D and S6).

It is known that the NF-κB signaling pathway plays a key role in the maintenance of DTX resistance, and the blockade of NF-κB can enhance the susceptibility of cancer cells to DTX (Kim et al., 2009) (O'Neill et al., 2011). Our laboratories have reported that the activity of NF-κB could be inhibited by the application of siRNA against RelA (a subunit of NF-κB) (Fitzgerald et al., 2016b) (Luan et al., 2019). In this study, CD.siRelA.PEG-FA significantly reduced the expression of RelA mRNA (~ 85% , $p < 0.01$) relative to CD.siRelA.PEG and CD.siNC.PEG-FA (Fig. 2E). Accordingly, the expression of RelA protein was significantly downregulated (~ 75%, $p < 0.01$) by CD.siRelA.PEG-FA as compared to the control groups (Fig. 2F and S7). These results confirm that the folate-targeted co-formulation was able to specifically co-deliver DTX and siRelA into CT26 cells, and the DTX-induced apoptotic effect was significantly enhanced by siRelA-mediated NF-κB blockade.

3.3. *In vivo* anti-CRC effects of folate-targeted co-formulation

The *in vivo* toxicity of folate-targeted co-formulation was evaluated in this study using healthy BALB/c mice (n = 4) (Fig. 3). As shown in Fig. 3A, no body weight loss was observed in mice following i.v. administration of the folate-targeted co-formulation relative to the saline group. The H&E staining results show that no histopathology was detected in the major organs (e.g., the heart, liver, spleen, lung and kidneys) of animals after i.v. injection of the folate-targeted co-formulation (Fig. 3B) as compared to the

saline group. Furthermore, no significant myelosuppression (Fig. 3C) or hepatic/renal injuries (Fig. 3D) were caused by the folate-targeted co-formulation compared with the saline group. These results indicate no systemic toxicity was caused by CD.DTX.siRelA.PEG-FA under the conditions tested.

The therapeutic efficacy of the folate-targeted co-formulation was assessed using the CT26-derived CRC mouse model (n = 5) (Fig. 4A). Results show that no significant tumor inhibition was achieved by free "DTX and siRelA" as compared to the saline. In contrast, tumor growth was significantly ($p < 0.05$) retarded by the non-targeted co-formulation relative to free "DTX and siRelA" (Fig. 4A), while anti-CRC efficacy was further ($p < 0.05$) enhanced by the folate-targeted co-formulation (Fig. 4A). In addition, no difference was found in the extent of apoptotic tumor cells between the saline and free "DTX and siRelA" (Fig. 4B). In contrast, CD.DTX.siRelA.PEG significantly increased apoptosis (~ 3%, $p < 0.05$) in tumor cells as compared to free "DTX and siRelA", while the folate-targeted co-formulation further ($p < 0.01$) improved the apoptotic efficacy (~17.5%) (Fig. 4B). As shown in Fig. 4C, 4D and S8, the folate-targeted co-formulation significantly ($p < 0.01$) reduced the expression of RelA mRNA (~ 80%) and protein (~ 75%) compared to any of the other groups. These results confirm that the anti-CRC efficacy resulted mainly from the cell-specific co-delivery of DTX and siRelA by the folate-targeted co-formulation.

4. Conclusions

An effective strategy to enhance the efficacy of DTX is still an unmet need for CRC therapy. Due to the role of NF-κB in the maintenance of DTX resistance (Kim et al., 2009) (O'Neill et al., 2011) and to the strong potential of siRNA to downregulate any gene of interest (Guo et al., 2010) (Guo et al., 2011), the application of siRNA

against NF-κB may improve the efficacy of DTX in the treatment of CRC. In this study, an amphiphilic cationic CD was used to develop a folate-targeted PEGylated delivery vector for co-formulating DTX and siRelA. The resultant co-formulation demonstrated favorable physicochemical properties, in terms of particle size (~ 125 nm), surface charge (~ 9 mV), drug loading (EE ≈ 89%; LC ≈ 11.8%), pH-triggered drug release (higher release in an acidic environment), and serum stability (no aggregation up to 24 h). These are compliant with the requirements for improved pharmacokinetic profiles. The *in vitro* studies, including cellular uptake, cytotoxicity, apoptosis and gene knockdown, confirmed that a synergistic therapeutic efficacy was achieved by cell-specific co-delivery of DTX and siRelA using the folate-targeted co-formulation. Following i.v. administration the inhibition of tumor growth detected for the combination of DTX and siRelA was achieved by the folate-targeted co-formulation, without causing significant toxicity. In addition, this formulation avoids the solvent related toxic effects of the current commercial formulation of DTK (Taxotere®) while still maintaining the ability to deliver a therapeutically relevant dose. These preliminary results indicate the future potential of this combination therapeutic strategy in the treatment of CRC.

Acknowledgements

J.G. acknowledges financial support from the Health Commission of Jilin Province, China (2020Q012), the Department of Education of Jilin Province, China (JJKH20190099KJ), the Outstanding Youth Foundation from the Department of Science and Technology of Jilin Province, China (20170520046JH), and Fundamental Research Funds for the Central Universities. C.M.O. acknowledges financial support from Science Foundation Ireland (SFI) co-funded under the European Regional

Development: 13/RC/2073 (Centre for Research in Medical Devices, CURAM); 12/RC/2275 (Synthesis and Solid State Cluster, SSPC), and 12/RC/2275 (Centre for Advanced Materials and BioEngineering Research, AMBER). Z.Y. acknowledges financial support from National Natural Science Foundation of China (81774240, 82074154) and Siming Scholar from Shanghai Shuguang Hospital (SGXZ-201904).

Conflicts of interest

Authors declare no conflict of interest.

Figure legends

Figure 1. Preparation and characterization of folate-targeted co-formulation. (A) The formulation schematic. (B) The binding efficiency of siRNA (0.5 μg) by co-formulations. (C) The particle size, PDI, surface charge, EE% and LC% of co-formulations (containing 1 μg siRNA) (n = 3). (D) TEM image of folate-targeted co-formulation (containing 1 μg siRNA) (bar = 100 nm). (E) The release of DTX from folate-targeted co-formulation (containing 500 μg DTX) in 0.01 M PBS (pH = 5.5 and 7.4) for 24 h at 37 oC (n = 4, * $p < 0.05$). (F) The particle size of folate-targeted co-formulation (containing 1 μg siRNA) in the presence of 50% serum-containing medium for 24 h at 37 oC (n = 4, * $p < 0.05$ and NS = no significance).

Figure 2. *In vitro* characterization of folate-targeted co-formulation. (A) Cellular uptake of CD.DTX.siFAM.PEG and CD.DTX.siFAM.PEG-FA (25 nM siFAM) was assessed using flow cytometry (n = 3). (B) Cell viability of CD.DTX.siRelA.PEG and CD.DTX.siRelA.PEG-FA (~ 1.33 μg/mL DTX and ~ 25 nM siRelA) (n = 3, * $p < 0.05$ and ** $p < 0.01$). (C) Cell viability of CD.siRelA.PEG-FA, CD.DTX.PEG-FA and

CD.DTX.siRelA.PEG-FA (~ 1.33 μg/mL DTX and ~ 25 nM siRelA) (n = 3, * $p < 0.05$ and ** $p < 0.01$). (D) Apoptotic cells (%) caused by CD.siRelA.PEG-FA, CD.DTX.PEG-FA and CD.DTX.siRelA.PEG-FA. (E) The mRNA level of RelA in CT26 cells following the treatment of CD.siRelA.PEG, CD.siNC.PEG-FA and CD.siRelA.PEG-FA (25 nM siRelA) (n = 3, * $p < 0.05$ and ** $p < 0.01$). (F) The protein level of RelA in CT26 cells following the treatment of CD.siRelA.PEG, CD.siNC.PEG-FA and CD.siRelA.PEG-FA (25 nM siRelA) (n = 3, * $p < 0.05$ and ** $p < 0.01$).

Figure 3. *In vivo* toxicity of folate-targeted co-formulation. (A) The body weight over 25 days following i.v. treatment of saline and folate-targeted co-formulation (~ 4 mg/kg DTX and ~ 1 mg/kg siRelA) on Day 1, 3 and 5 (n = 4). (B) The organs were collected on Day 25 and assessed using H&E staining assay. No significant toxicity was caused by the folate-targeted co-formulation as compared to saline. (C) Hematological analysis including red blood cells (RBCs), white blood cells (WBCs), platelets (PLTs) and hemoglobin (HGB), carried out on Day 25 (n = 4). (D) The liver/kidney functions including alanine aminotransferase (ALT), aspartate aminotransferase (AST), blood urea nitrogen (BUN) and creatinine (CRE), determined on Day 25 (n = 4).

Figure 4. *In vivo* antitumor activity of folate-targeted co-formulation. (A) Tumor growth of CRC following the treatment of saline, free "DTX and siRelA", CD.DTX.siRelA.PEG and CD.DTX.siRelA.PEG-FA (~ 4 mg/kg DTX and ~ 1 mg/kg siRelA) over a 35-day period (n = 5, * $p < 0.05$ and NS = no significance). (B) Apoptosis (%) in tumor tissues was examined on Day 7 by TUNEL Cell Apoptosis Kit (n = 4, * $p < 0.05$ and ** $p < 0.01$). (C) mRNA expression level of RelA in tumor tissues following the treatment of folate-targeted co-formulation on Day 7 (n = 4, ** $p < 0.01$ and NS = no significance). (D) Protein expression level of RelA in tumor tissues following the treatment of folate-targeted co-formulation on Day 7.

References

Bowerman, C.J., Byrne, J.D., Chu, K.S., Schorzman, A.N., Keeler, A.W., Sherwood, C.A., Perry, J.L., Luft, J.C., Darr, D.B., Deal, A.M., Napier, M.E., Zamboni, W.C., Sharpless, N.E., Perou, C.M., DeSimone, J.M., 2017. Docetaxel-Loaded PLGA Nanoparticles Improve Efficacy in Taxane-Resistant Triple-Negative Breast Cancer. Nano Lett 17, 242-248.

Bray, F., Ferlay, J., Soerjomataram, I., Siegel, R.L., Torre, L.A., Jemal, A., 2018. Global cancer statistics 2018: GLOBOCAN estimates of incidence and mortality worldwide for 36 cancers in 185 countries. CA Cancer J Clin 68, 394-424.

Chi, C.L., Li, F.W., Liu, H.B., Feng, S.Y., Zhang, Y.J., Zhou, D., Zhang, R.K., 2019. Docetaxel-loaded biomimetic nanoparticles for targeted lung cancer therapy in vivo. J Nanopart Res 21.

Dekker, E., Tanis, P.J., Vleugels, J.L.A., Kasi, P.M., Wallace, M.B., 2019. Colorectal cancer. The Lancet 394, 1467-1480.

Esmaeili, F., Ghahremani, M.H., Ostad, S.N., Atyabi, F., Seyedabadi, M., Malekshahi, M.R., Amini, M., Dinarvand, R., 2008. Folate-receptor-targeted delivery of docetaxel nanoparticles prepared by PLGA-PEG-folate conjugate. J Drug Target 16, 415-423.

Esmaeli, B., Valero, V., Ahmadi, M.A., Booser, D., 2001. Canalicular stenosis secondary to docetaxel (taxotere): a newly recognized side effect. Ophthalmology 108, 994-995.

Evans, J.C., Malhotra, M., Fitzgerald, K.A., Guo, J., Cronin, M.F., Curtin, C.M., O'Brien, F.J., Darcy, R., O'Driscoll, C.M., 2017. Formulation and Evaluation of Anisamide-Targeted Amphiphilic Cyclodextrin Nanoparticles To Promote Therapeutic Gene Silencing in a 3D Prostate Cancer Bone Metastases Model. Mol Pharm 14, 42-52.

Evans, J.C., Malhotra, M., Guo, J., O'Shea, J.P., Hanrahan, K., O'Neill, A., Landry, W.D., Griffin, B.T., Darcy, R., Watson, R.W., O'Driscoll, C.M., 2016. Folate-targeted amphiphilic cyclodextrin.siRNA nanoparticles for prostate cancer therapy exhibit PSMA mediated uptake, therapeutic gene silencing in vitro and prolonged circulation in vivo. Nanomedicine 12, 2341-2351.

Fani, M., Tamma, M.L., Nicolas, G.P., Lasri, E., Medina, C., Raynal, I., Port, M., Weber, W.A., Maecke, H.R., 2012. In vivo imaging of folate receptor positive tumor xenografts using novel 68Ga-NODAGA-folate conjugates. Mol Pharm 9, 1136-1145.

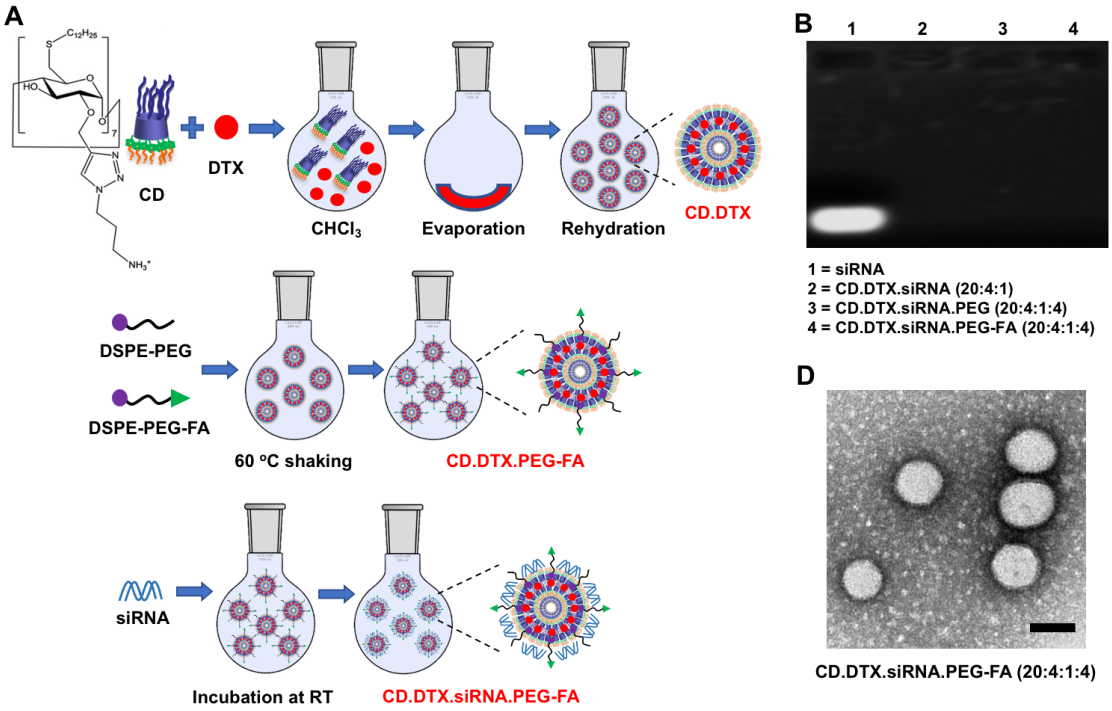
Ferraresi, V., Milella, M., Vaccaro, A., D'Ottavio, A.M., Papaldo, P., Nistico, C., Thorel, M.F., Marsella, A., Carpino, A., Giannarelli, D., Terzoli, E., Cognetti, F., 2000. Toxicity and activity of docetaxel in anthracycline-pretreated breast cancer patients: a phase II study. Am J Clin Oncol 23, 132-139.

Ferrati, S., Nicolov, E., Bansal, S., Hosali, S., Landis, M., Grattoni, A., 2015. Docetaxel/2-Hydroxypropyl beta -Cyclodextrin Inclusion Complex Increases Docetaxel Solubility and Release from a Nanochannel Drug Delivery System. Curr Drug Targets 16, 1645-1649.

Fitzgerald, K.A., Guo, J., Raftery, R.M., Castano, I.M., Curtin, C.M., Gooding, M., Darcy, R., FJ, O.B., CM, O.D., 2016a. Nanoparticle-mediated siRNA delivery assessed in a 3D co-culture model simulating prostate cancer bone metastasis. Int J Pharm 511, 1058-1069.
Fitzgerald, K.A., Guo, J., Tierney, E.G., Curtin, C.M., Malhotra, M., Darcy, R., O'Brien, F.J., O'Driscoll, C.M., 2015. The use of collagen-based scaffolds to simulate prostate cancer bone metastases with potential for evaluating delivery of nanoparticulate gene therapeutics. Biomaterials 66, 53-66.
Fitzgerald, K.A., Rahme, K., Guo, J., Holmes, J.D., O'Driscoll, C.M., 2016b. Anisamide-targeted gold nanoparticles for siRNA delivery in prostate cancer - synthesis, physicochemical characterisation and in vitro evaluation. J Mater Chem B 4, 2242-2252.
Gao, W., Chan, J.M., Farokhzad, O.C., 2010. pH-Responsive nanoparticles for drug delivery. Mol Pharm 7, 1913-1920.
Godinho, B.M., Ogier, J.R., Darcy, R., O'Driscoll, C.M., Cryan, J.F., 2013. Self-assembling modified beta-cyclodextrin nanoparticles as neuronal siRNA delivery vectors: focus on Huntington's disease. Mol Pharm 10, 640-649.
Guo, J., Bourre, L., Soden, D.M., O'Sullivan, G.C., O'Driscoll, C., 2011. Can non-viral technologies knockdown the barriers to siRNA delivery and achieve the next generation of cancer therapeutics? Biotechnol Adv 29, 402-417.
Guo, J., Cheng, W.P., Gu, J., Ding, C., Qu, X., Yang, Z., O'Driscoll, C., 2012a. Systemic delivery of therapeutic small interfering RNA using a pH-triggered amphiphilic poly-L-lysine nanocarrier to suppress prostate cancer growth in mice. Eur J Pharm Sci 45, 521-532.
Guo, J., Fisher, K.A., Darcy, R., Cryan, J.F., O'Driscoll, C., 2010. Therapeutic targeting in the silent era: advances in non-viral siRNA delivery. Mol Biosyst 6, 1143-1161.
Guo, J., Huang, L., 2020. Membrane-core nanoparticles for cancer nanomedicine. Adv Drug Deliv Rev 156, 23-39.
Guo, J., Ogier, J.R., Desgranges, S., Darcy, R., O'Driscoll, C., 2012b. Anisamide-targeted cyclodextrin nanoparticles for siRNA delivery to prostate tumours in mice. Biomaterials 33, 7775-7784.
Guo, J., Russell, E.G., Darcy, R., Cotter, T.G., McKenna, S.L., Cahill, M.R., O'Driscoll, C.M., 2017. Antibody-Targeted Cyclodextrin-Based Nanoparticles for siRNA Delivery in the Treatment of Acute Myeloid Leukemia: Physicochemical Characteristics, in Vitro Mechanistic Studies, and ex Vivo Patient Derived Therapeutic Efficacy. Mol Pharm 14, 940-952.
Guo, J., Yu, Z., Das, M., Huang, L., 2020. Nano Codelivery of Oxaliplatin and Folinic Acid Achieves Synergistic Chemo-Immunotherapy with 5-Fluorouracil for Colorectal Cancer and Liver Metastasis. ACS Nano 14, 5075-5089.
Gustavsson, B., Carlsson, G., Machover, D., Petrelli, N., Roth, A., Schmoll, H.J., Tveit, K.M., Gibson, F., 2015. A review of the evolution of systemic chemotherapy in the management of colorectal cancer. Clin Colorectal Cancer 14, 1-10.
He, Y., Luo, L., Liang, S., Long, M., Xu, H., 2017. Amino-functionalized mesoporous silica nanoparticles as efficient carriers for anticancer drug delivery. J Biomater Appl 32, 524-532.

Huang, X.X., Zhou, C.L., Wang, H., Chen, C., Yu, S.Q., Xu, Q., Zhu, Y.Y., Ren, Y., 2011. Pharmacokinetics, efficacy, and safety evaluation of docetaxel/hydroxypropyl-sulfobutyl-beta-cyclodextrin inclusion complex. AAPS PharmSciTech 12, 665-672.
Joshi, U., Filipczak, N., Khan, M.M., Attia, S.A., Torchilin, V., 2020. Hypoxia-sensitive micellar nanoparticles for co-delivery of siRNA and chemotherapeutics to overcome multi-drug resistance in tumor cells. Int J Pharm 590, 119915.
Kim, S.M., Lee, S.Y., Yuk, D.Y., Moon, D.C., Choi, S.S., Kim, Y., Han, S.B., Oh, K.W., Hong, J.T., 2009. Inhibition of NF-kappaB by ginsenoside Rg3 enhances the susceptibility of colon cancer cells to docetaxel. Arch Pharm Res 32, 755-765.
Labala, S., Jose, A., Chawla, S.R., Khan, M.S., Bhatnagar, S., Kulkarni, O.P., Venuganti, V.V.K., 2017. Effective melanoma cancer suppression by iontophoretic co-delivery of STAT3 siRNA and imatinib using gold nanoparticles. Int J Pharm 525, 407-417.
Liu, Y.T., Li, K., Pan, J., Liu, B., Feng, S.S., 2010. Folic acid conjugated nanoparticles of mixed lipid monolayer shell and biodegradable polymer core for targeted delivery of Docetaxel. Biomaterials 31, 330-338.
Luan, X., Rahme, K., Cong, Z., Wang, L., Zou, Y., He, Y., Yang, H., Holmes, J.D., O'Driscoll, C.M., Guo, J., 2019. Anisamide-targeted PEGylated gold nanoparticles designed to target prostate cancer mediate: Enhanced systemic exposure of siRNA, tumour growth suppression and a synergistic therapeutic response in combination with paclitaxel in mice. Eur J Pharm Biopharm 137, 56-67.
McCarthy, J., O'Neill, M.J., Bourre, L., Walsh, D., Quinlan, A., Hurley, G., Ogier, J., Shanahan, F., Melgar, S., Darcy, R., O'Driscoll, C.M., 2013. Gene silencing of TNF-alpha in a murine model of acute colitis using a modified cyclodextrin delivery system. J Control Release 168, 28-34.
Nikkhoo, A., Rostami, N., Farhadi, S., Esmaily, M., Moghadaszadeh Ardebili, S., Atyabi, F., Baghaei, M., Haghnavaz, N., Yousefi, M., Aliparasti, M.R., Ghalamfarsa, G., Mohammadi, H., Sojoodi, M., Jadidi-Niaragh, F., 2020. Codelivery of STAT3 siRNA and BV6 by carboxymethyl dextran trimethyl chitosan nanoparticles suppresses cancer cell progression. Int J Pharm 581, 119236.
O'Mahony, A.M., Godinho, B.M., Ogier, J., Devocelle, M., Darcy, R., Cryan, J.F., O'Driscoll, C.M., 2012. Click-modified cyclodextrins as nonviral vectors for neuronal siRNA delivery. ACS Chem Neurosci 3, 744-752.
O'Neill, A.J., Prencipe, M., Dowling, C., Fan, Y., Mulrane, L., Gallagher, W.M., O'Connor, D., O'Connor, R., Devery, A., Corcoran, C., Rani, S., O'Driscoll, L., Fitzpatrick, J.M., Watson, R.W., 2011. Characterisation and manipulation of docetaxel resistant prostate cancer cell lines. Mol Cancer 10, 126.
Pazdur, R., Lassere, Y., Soh, L.T., Ajani, J.A., Bready, B., Soo, E., Sugarman, S., Patt, Y., Abbruzzese, J.L., Levin, B., 1994. Phase II trial of docetaxel (Taxotere) in metastatic colorectal carcinoma. Ann Oncol 5, 468-470.
Quaglia, F., Ostacolo, L., Mazzaglia, A., Villari, V., Zaccaria, D., Sciortino, M.T., 2009. The intracellular effects of non-ionic amphiphilic cyclodextrin nanoparticles in the delivery of anticancer drugs. Biomaterials 30, 374-382.
Rahme, K., Guo, J., Holmes, J.D., O'Driscoll, C.M., 2015. Evaluation of the physicochemical properties and the biocompatibility of polyethylene glycol-conjugated

gold nanoparticles: A formulation strategy for siRNA delivery. Colloids Surf B Biointerfaces 135, 604-612.
Rothdiener, M., Muller, D., Castro, P.G., Scholz, A., Schwemmlein, M., Fey, G., Heidenreich, O., Kontermann, R.E., 2010. Targeted delivery of SiRNA to CD33-positive tumor cells with liposomal carrier systems. J Control Release 144, 251-258.
Sternberg, C.N., ten Bokkel Huinink, W.W., Smyth, J.F., Bruntsch, V., Dirix, L.Y., Pavlidis, N.A., Franklin, H., Wanders, S., Le Bail, N., Kaye, S.B., 1994. Docetaxel (Taxotere), a novel taxoid, in the treatment of advanced colorectal carcinoma: an EORTC Early Clinical Trials Group Study. Br J Cancer 70, 376-379.
Suk, J.S., Xu, Q.G., Kim, N., Hanes, J., Ensign, L.M., 2016. PEGylation as a strategy for improving nanoparticle-based drug and gene delivery. Adv Drug Deliver Rev 99, 28-51.
Taniguchi, K., Karin, M., 2018. NF-kappaB, inflammation, immunity and cancer: coming of age. Nat Rev Immunol 18, 309-324.
Wang, Q., Alshaker, H., Bohler, T., Srivats, S., Chao, Y., Cooper, C., Pchejetski, D., 2017. Core shell lipid-polymer hybrid nanoparticles with combined docetaxel and molecular targeted therapy for the treatment of metastatic prostate cancer. Sci Rep 7, 5901.
Yu, Z., Guo, J., Hu, M., Gao, Y., Huang, L., 2020. Icaritin Exacerbates Mitophagy and Synergizes with Doxorubicin to Induce Immunogenic Cell Death in Hepatocellular Carcinoma. ACS Nano 14, 4816-4828.



C

Formulation	WR of CD:DTX:siRNA:PEG-(FA)	Diameter (nm)	PDI	Zeta Potential (mV)	EE (%)	LC (%)
CD.DTX.siRNA	20:4:1	100 ± 4	0.24	40 ± 3	89 ± 4	14.2 ± 0.6
CD.DTX.siRNA.PEG	20:4:1:4	122 ± 6	0.26	10 ± 4	90 ± 5	12.2 ± 0.4
CD.DTX.siRNA.PEG-FA	20:4:1:4	125 ± 5	0.27	9 ± 3	89 ± 4	11.8 ± 0.6

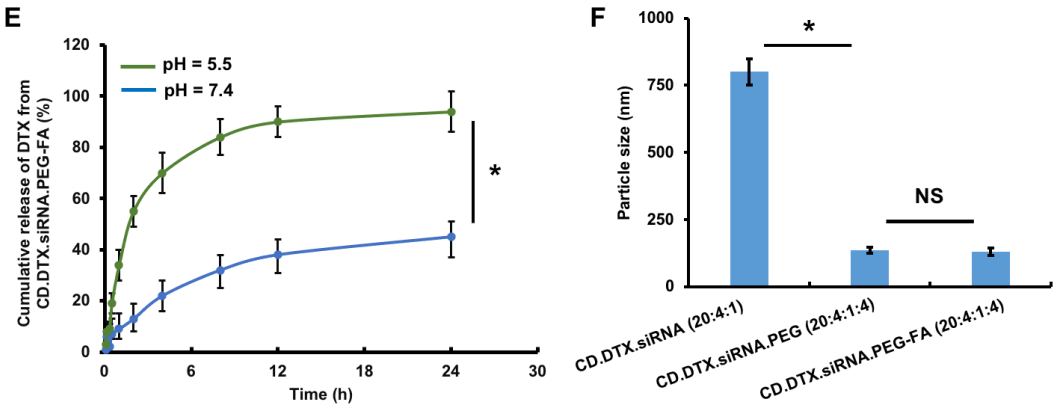


Figure 1.

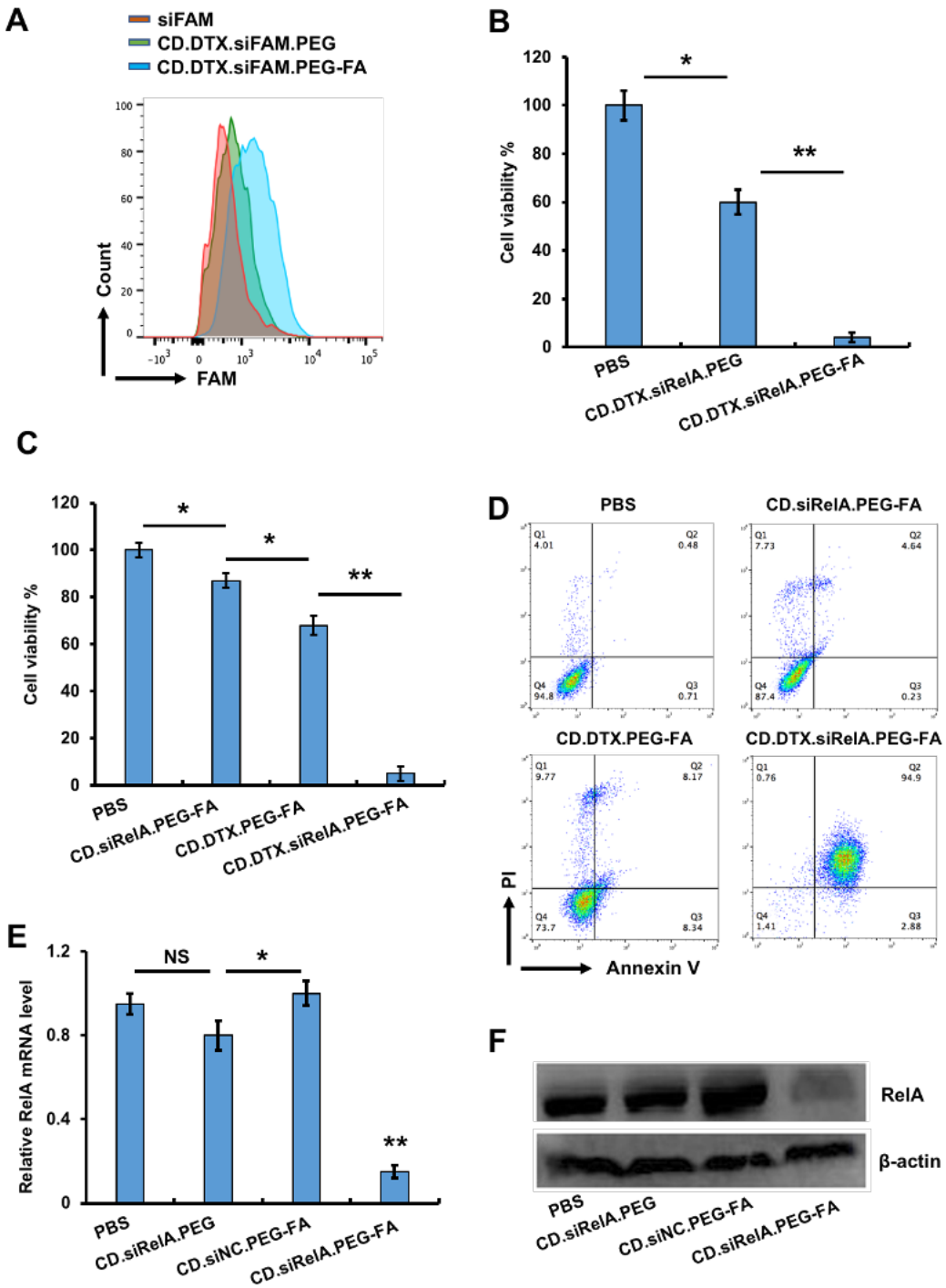

A
siFAM
CD.DTX.siFAM.PEG
CD.DTX.siFAM.PEG-FA
Count
FAM
B
Cell viability %
PBS
CD.DTX.siRelA.PEG
CD.DTX.siRelA.PEG-FA
C
Cell viability %
PBS
CD.siRelA.PEG-FA
CD.DTX.PEG-FA
CD.DTX.siRelA.PEG-FA
D
PBS
CD.siRelA.PEG-FA
CD.DTX.PEG-FA
CD.DTX.siRelA.PEG-FA
PI
Annexin V
E
Relative RelA mRNA level
NS
PBS
CD.siRelA.PEG
CD.siNC.PEG-FA
CD.siRelA.PEG-FA
F
RelA
β-actin
PBS
CD.siRelA.PEG
CD.siNC.PEG-FA
CD.siRelA.PEG-FA

Figure 2.

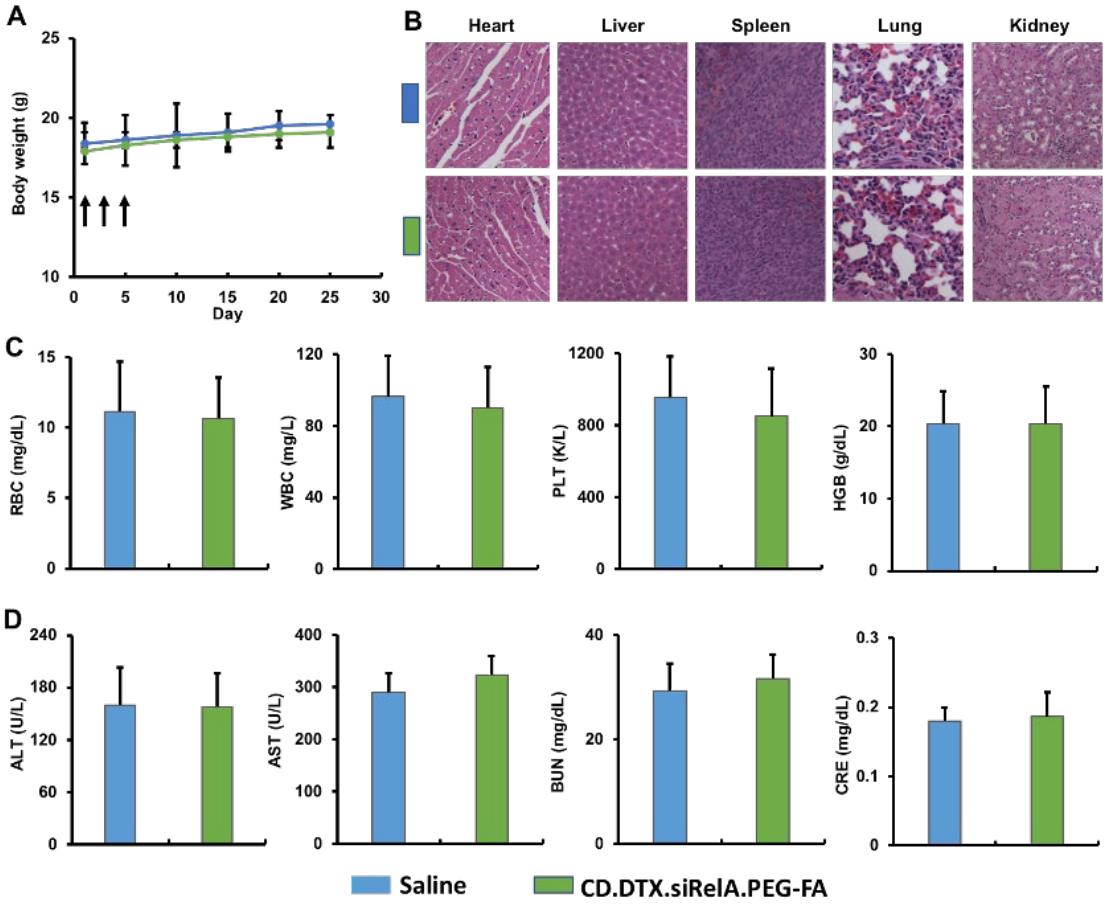

A
Body weight (g)
Day
B
Heart
Liver
Spleen
Lung
Kidney
C
RBC (mg/dL)
WBC (mg/L)
PLT (K/L)
HGB (g/dL)
D
ALT (U/L)
AST (U/L)
BUN (mg/dL)
CRE (mg/dL)
Saline
CD.DTX.siRelA.PEG-FA

Figure 3.

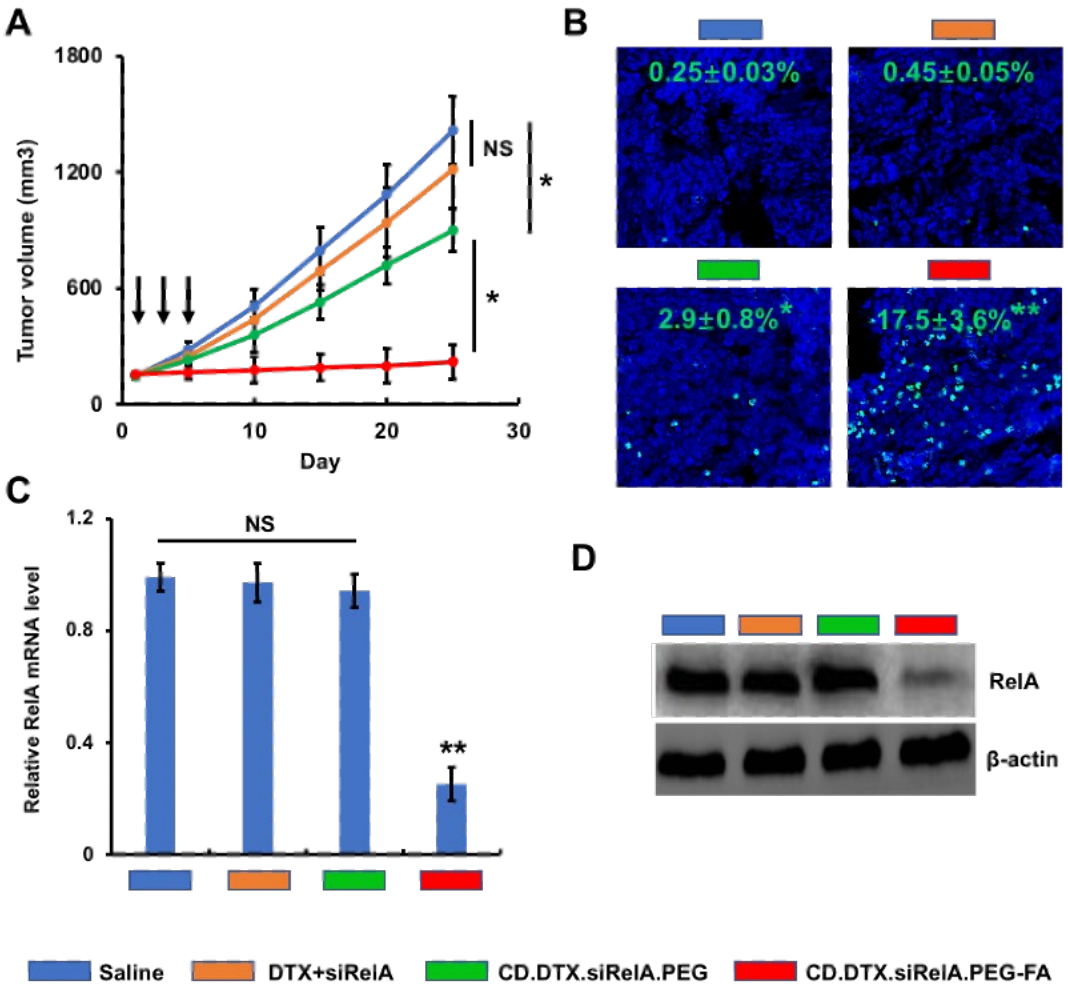

A
1800
1200
600
0
Tumor volume (mm3)
0
10
20
30
Day
NS
*
*
B
0.25±0.03%
0.45±0.05%
2.9±0.8%*
17.5±3.6%**
C
1.2
0.8
0.4
0
Relative RelA mRNA level
NS
**
D
RelA
β-actin
Saline
DTX+siRelA
CD.DTX.siRelA.PEG
CD.DTX.siRelA.PEG-FA

Figure 4.